Journal of Flood Risk Management

WILEY

CIWEM Chartered Institution of Water and Environmental Management | Journal of Flood Risk Management

ORIGINAL ARTICLE OPEN ACCESS

Operational Reliability of Emergency Measures, a Case Study for the BresDefender

D. Janssen[1,2] | S. N. Jonkman[1] | A. J. M. Schmets[2] | B. Hofland[1] | E. Dado[2]

[1]Department of Hydraulic Structures and Flood Risk, Delft University of Technology, Delft, the Netherlands | [2]Netherlands Defence Academy, The Hague, the Netherlands

Correspondence: D. Janssen (d.janssen@tudelft.nl)

Received: 4 April 2024 | **Revised:** 31 December 2024 | **Accepted:** 3 March 2025

Funding: This work was supported by the Ministerie van Defensie.

Keywords: disaster risk reduction | embankments and levees | emergency management | flood defence measures

ABSTRACT

During extreme high-water events in river systems, the load on a levee section may exceed its resistance, initiating the breaching process which eventually leads to levee failure. The success of an emergency measure to intervene in the initial phases of levee failure is mainly dependent on its timely application. Quick action is required to prepare and deploy an emergency measure before damages to the levee section have become irreparable. In this study, we investigate the key parameters for successful application of an emergency measure, focusing on the BresDefender case study. The BresDefender is a floating pontoon used by the Dutch military, which is intended to avoid or postpone levee failure. A model has been developed taking the operational steps in the implementation of the emergency measure during a high water and the (uncertainty) in the duration of these processes into account. The model is used to quantify the probability of successful operation to prevent levee failure due to overflow or slope instability. The probability of successful application of the BresDefender has been simulated for river flood situations in the Netherlands. For the river Rhine, where the examined cases were prone to slope instabilities, the probability of arriving in time was found to be 70%. But for the Meuse case, where the examined cases were prone to overflow, the probability of arriving in time was found to be only 0%. The critical steps in the process after the occurrence of damage to the levee are damage detection, the decision to repair the damage, the transport of the emergency measure, and the placement of the measure. By incorporating emergency measures in emergency preparedness procedures, the time required for the critical steps will be decreased and the probability of successful application of the emergency measure, i.e., its contribution to flood risk reduction, will be enhanced.

1 | Introduction

Levee systems play a critical role in safeguarding both lives and infrastructure from the devastating impacts of flooding. While these systems accept a small risk of flooding, the potential consequences in terms of loss of life and damage from an actual flood are severe (Jonkman 2007). Additionally, the anticipated increase in loads on the levee system, driven by climate change (Kundzewicz et al. 2013), calls for measures to enhance its resilience. One way to address these challenges is the implementation of emergency response measures for floods. This study exclusively focuses on the application of emergency response measures. These measures are intended to mitigate unforeseen circumstances, for which the required quantity and location of application are not known beforehand (Delfland 2011; Knotter and Krikke 2021).

Successful application of emergency measures relies on several critical aspects: detection of the weak spot that has to be reinforced, timely deployment at the required location, safe conditions to properly place the emergency measure safeguarding people positioning the measure, and sufficient structural

FIGURE 1 | BresDefender prototype as applied during large-scale experiments in the Hedwige-Prosperpolder (March, 2022).

resistance (Lendering 2018). Both the time required to implement the emergency measure as well as the time available to failure of a levee are subject to uncertainty.

In this study, we develop a probabilistic model that aims to identify the likelihood of an effective application of emergency measures. Here, successful application of the emergency measure means that the failure process is interrupted and the water retaining function of the levee is maintained. The results obtained from this study will contribute to a more informed decision-making process and better preparation, ultimately improving the probability of successful application of emergency measures.

Then the probabilistic model is implemented in a case study featuring the emergency response measure BresDefender. The BresDefender is a military pontoon, normally applied to construct temporary floating bridges (Figure 1). In this context, the BresDefender is used to stop the breaching process in its early phases by locally reinforcing a weakened levee section (Janssen et al. 2021). Application of the BresDefender prevents or delays a levee breach caused by overflow. The system can also contribute to reducing the risk of slope instability, as it influences the phreatic line inside the levee. An advantage of the BresDefender is its ability to be transported and applied from the water, eliminating the requirement for heavy equipment on the levee.

In this paper, first a comprehensive theoretical framework is presented, providing an overview of the steps in the proposed probabilistic model (Section 2). This is followed by detailing the estimates of the time available (until breaching) in Section 3 and the time required to implement measures in emergency response situations in Section 4. These times, with their corresponding uncertainty interval, are input to the overall model as presented in Section 2. To estimate the uncertainty in the time required, an expert judgment analysis among Dutch water managers has been conducted following the classical model of Cooke (1991). Subsequently, an expert judgment analysis, with the input of Dutch water experts, is conducted and presented

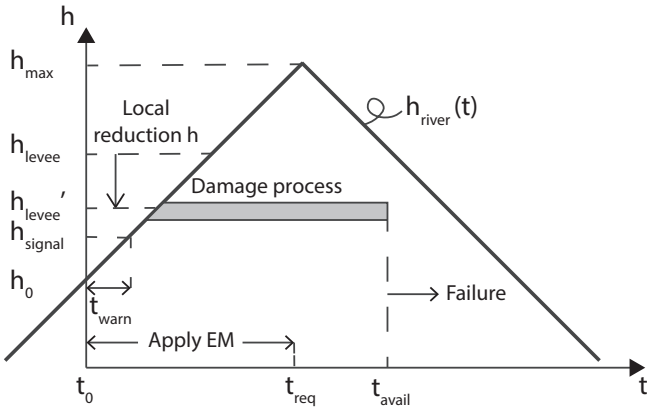

FIGURE 2 | Flood water wave with time required (t_{req}) to place an emergency measure (EM) and time available (t_{avail}), for scenario with local reduction crest level (from h_{levee} to h_{levee}'). The thick solid line symbolizes an arbitrary high water wave (h_{river}), with a maximum water level h_{max}. The signal water level h_{signal}, is the water level at a certain agreed threshold level. The time available between issuing a state of emergency and exceeding the water level threshold is equal to t_{warn}.

in Section 4.2, offering insights into the time requirements. Hereafter, the probabilistic model is used for two different case studies—one describing a levee in the Rhine basin and one in the Meuse (Section 5).

2 | General Model Framework

The leading parameters for the application of an emergency measure are time (t) and damage, resulting from a characteristic elevation level (h) (Janssen et al. 2021). These levels are separated into the water level in the river, $h_{river}(t)$, with the maximum water level h_{max}, and the water retaining height of the levee, h_{levee}. These parameters are plotted on the axes in Figure 2. The time is separated into a time required to apply an emergency measure, t_{req} and the time available before failure of the levee, t_{avail}.

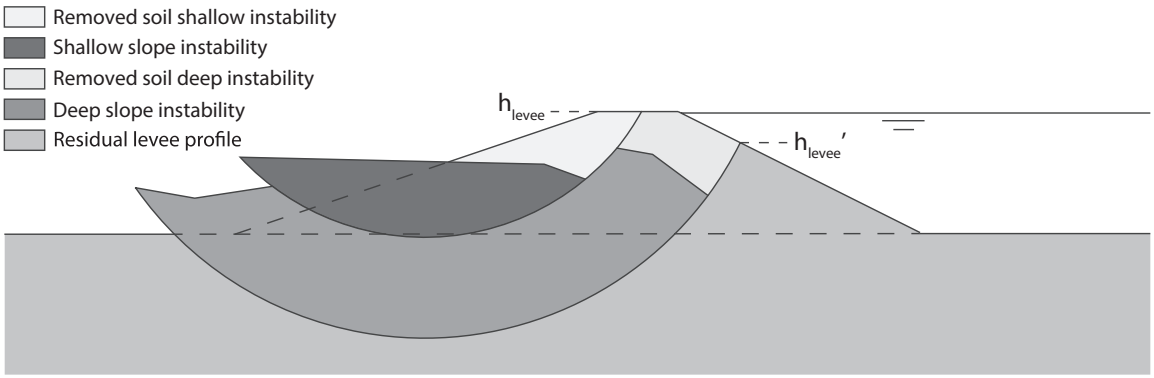

FIGURE 3 | Definition of slope instability, where a shallow instability did not lead to a reduction of the crest height while a deep instability did; these circles could either occur sequentially or independently.

The emergency response process starts if the water authorities issue a state of emergency, at time t_0, with corresponding river water level h_0. This state of emergency is issued if the water level in the river is predicted to exceed a certain agreed threshold level (h_{signal}) within a certain amount of time. The time available between issuing a state of emergency and exceeding the water level threshold is equal to t_{warn}. This warning time depends on the predictive accuracy of water level forecast systems installed by the local water authority (MinIenM 2022).

In case the water level in the river exceeds the maximum retaining height of the levee, h_{levee}, the damage process starts. The time available, t_{avail}, is the time from issuing a state of emergency until the damages to a specific levee section are not repairable by the considered emergency measure. This is the case when the dimensions of the damage to the levee (the breach dimensions) are larger than the physical application limits of the emergency measure itself, or if the emergency measure cannot be placed without the risk of serious harm to the people involved in construction of the measure. The installation of the emergency measure is too late if the required time is larger than the available time.

No overflow occurs if the maximum water level in the river, h_{max}, is smaller than the levee height, h_{levee}. The levee failure starts when the loads on the levee has become larger than its resistance. The failure process can consist of several internal and external processes, which may enhance each other, ultimately leading to failure of the levee (Van et al. 2022). In the model that is presented here, a failure process is a crest height reduction caused by (successive) slope instabilities. This failure process reduces the crest height from h_{levee} to h_{levee}', Figure 3. This failure mechanism may be triggered by accumulation of pore water in the levee over time (Schiereck 1998). It is important to note that a single, more shallow failure plane may not cause an immediate reduction in crest height, as a slope instability may not extend all the way to the crest, see Figure 3 (Remmerswaal et al. 2021; Van Der Krogt et al. 2019).

Application of an emergency measure during a flood wave can have several effects on the failure process (Figure 4). Application of an emergency measure will increase the water retaining level with an extra height, h_{EM}. Then either of two scenarios may occur. In scenario 1, the maximum water level in the river (h_{max})

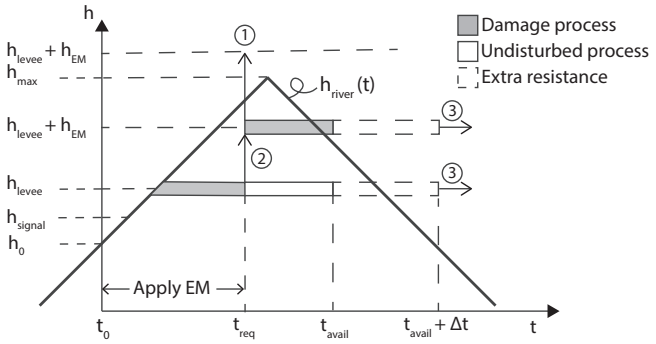

FIGURE 4 | Three possible scenarios for the application of an emergency measure (EM) within a flood water wave. The thick solid line symbolizes an arbitrary high water wave. In scenario 1 the sum of h_{levee} and h_{EM} is larger than the maximum water level, h_{max}. In sicario 2, the sum of h_{levee} and h_{EM} is smaller than the maximum water level, h_{max}. In scenario 3, the emergency measure increases the resistance of the levee and herewith the time to failure.

will be lower than the height of the levee with the emergency measure. In this scenario the damage process is successfully arrested. In scenario 2, the combined levee and emergency measure height are lower than the maximum water level in the river, hence the damage process will continue, however it may develop at a slower pace.

Next to increasing the levee height, the placement of an emergency measure may also extend the time available until failure (Δt), either by reducing the head of the flow, or by increasing the erosion resistance of the levee and its soil (scenario 3). Application of the emergency measure is assumed to be successful if the water level in the river decreases below the (temporarily increased) levee height, before the levee had reached complete failure.

The BresDefender case study only considers scenarios 1 and 2, omitting scenario 3 to simplify the analysis. In practice, the BresDefender may enhance damage resistance as well as (scenario 3) real scale experiments with the BresDefender prototype showed a significant reduction in water flowing through the breach (Maat et al. 2023). It was found that the reduction in flow rate through the breach decreases the erosion rate of soil and herewith increases the breaching time.

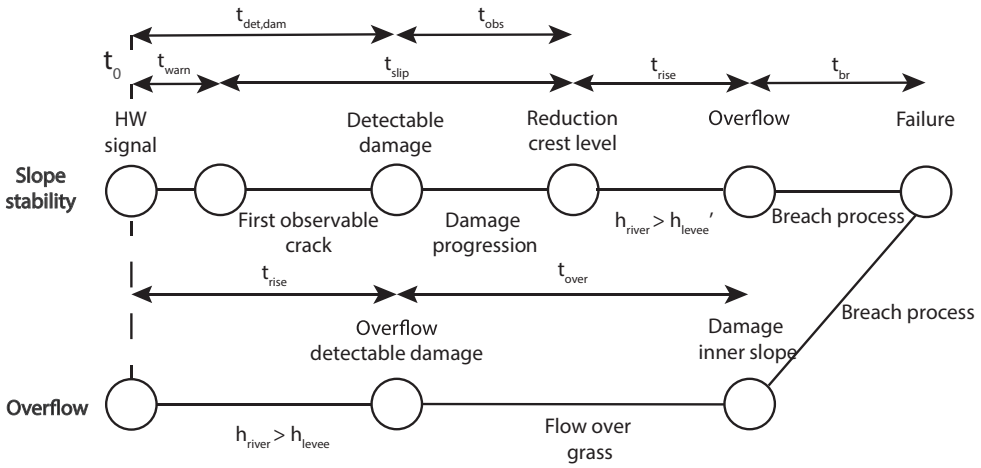

FIGURE 5 | Sequence of failure process events caused by flow over grass inner slope and overtopping in which circles represent space–time events. High water (HW) signal corresponds to t_0. Symbols are introduced in coming paragraphs.

3 | Damage Process: Time Available

3.1 | General

Now, the time available until levee failure, t_{avail} (see Figures 3 and 4), will be elaborated. In further developing the model, two failure processes are to be considered, one for failure caused by overflow (Figure 5) and one for failure by slope instability (Figure 5). In the overflow failure process (Figure 5), the water level of the river initially rises, leading to overflow of the levee. From this moment onwards, observable damage is assumed within the model. This continuous overflow will cause damage to the inner slope, exposing the sand core of the levee to the water flow. Then, the breaching process starts, followed by failure of the levee when the erosion has reached the outer crest line.

The failure path for slope instabilities starts with the occurrence of a single deformation in the levee cross section. After this moment, the damage can be visibly observed. This deformation process is continuous, ultimately leading to a crest height reduction. After that, water will rise until the water level in the river becomes higher than the reduced crest level. Lastly, the breaching process starts as soon as water starts to flow over the levee, ending up at the failure of the levee (Figure 5). Each of these sequential steps within both failure processes will be elaborated on in more detail below.

3.2 | Overflow

The time of overflow (t_{over}) is defined as the interval between the moment of initial overflow of the levee and the time of occurrence of damage to the protective grass layer. Once damage has occurred in the grass layer, a new phase set in, the actual breaching process, t_{br}. The overflowing water exerts a shear stress on the protective grass layer. The resistance of the grass against this shear is quantified as the overflow velocity sustained over a specific duration (Hewlett et al. 1985), depending on the quality of the grass. This quality is categorized as good, normal or poor. The interdependence between the mentioned parameters is illustrated in Figure 6.

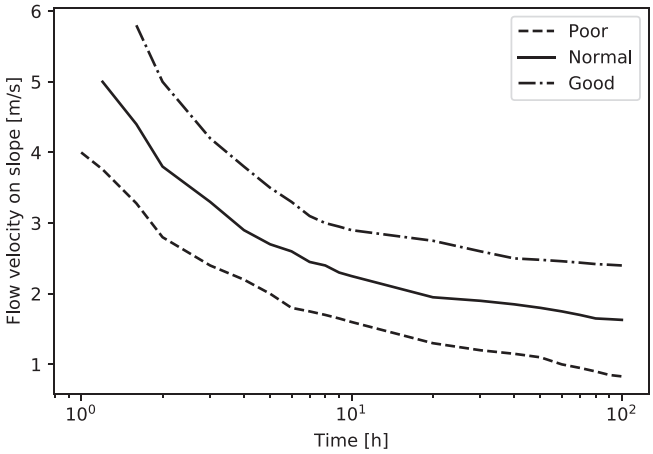

FIGURE 6 | Time to failure of protective grass layer of a certain quality as a function of maximum flow velocity on the inner slope of the levee (Hewlett et al. 1985).

The velocity on the outer levee slope can be determined using the Manning equation (Equation 1). Here, N is the Manning coefficient, set to 0.03 (Hewlett et al. 1985); R is the hydraulic radius of the flow, configured for a flow width of 1 m; S denotes the slope of the energy line, adjusted to a slope of 1:3, equal to the slope on which the BresDefender has been tested. Pressure head is the difference between the maximum water level in the river and the levee height.

$$v = \frac{1}{N} R^{\frac{2}{3}} s^{\frac{1}{2}} \tag{1}$$

Based on the expected velocity (Equation 1), the time to failure of poor and good quality grass cover can be obtained from Figure 6. The time-to-failure of the poor and good quality protective grass layer, given the determined flow velocity, will serve as lower and upper bound in the probabilistic model. In the simulation, time of overflow (t_{over}) is randomly selected within the bounds, based on a uniform distribution. In situations where the velocity falls outside the available data range, the time-to-failure is set to the smallest or largest values within the available dataset.

3.3 | Slope Instability

The model integrates the probability of the occurrence of slope instability corresponding to a specific river water level, utilizing a site-specific fragility curve, as available from a Dutch database (Kolen et al. 2021), and elaborated on in the section case studies. The time until reduction of the crest height (t_{slip}) is approximated and linked to the flood water wave, as illustrated in Figure 7. The asymmetric normalized distribution of the time required for the first failure is centered around the peak of the flood water wave (t_{max}). A standard deviation for both the left and the right side of the peak is equal to 1/3 of the time differential between t_{warn} and t_{max}. These boundaries are selected, acknowledging a small probability of slope instabilities at t_{warn} in site-specific fragility curves. For the Dutch case, this signal water level threshold is exceeded 1/50 years (MinIenM 2022).

A levee starts to show visible damage, before a total crest height reduction, in the form of cracks and soil deformation. The time of observable damage, t_{obs}, is the time interval between the moment of first visible damage and total crest height reduction. The time of observable damage is estimated as a value between 0 and 18 in a uniform distribution. Here the lower limit of t_{obs} is 0 is known to be a conservative assumption. The upper limit is determined using data of real levee failure occurrences at Breitenhagen (Kool et al. 2019) and Fishbeck (Henning and Jüpner 2015). Here detectable damage was observed 12 and 17, respectively before levee failure. The time to detectable damage, $t_{det,dam}$, is the time between the high water signal and the first observable damage, and is defined in (Equation 2).

$$t_{det,dam} = t_{warn} + t_{slip} - t_{obs} \quad (2)$$

The crest height reduction of the levee is randomly assigned as a value ranging from 0.5 to 2 m, after the occurrence of a slip failure. This is based on reported slip failures, which showed a crest height reduction of 1–2 m, as indicated by t Hart et al. (2016). Recent levee failure cases at Fishbeck (Henning and Jüpner 2015) showed a crest height reduction of 0.5 m, and while a reduction of 1 m was observed at Breitenhagen shortly after overflow (Brauneck et al. 2016).

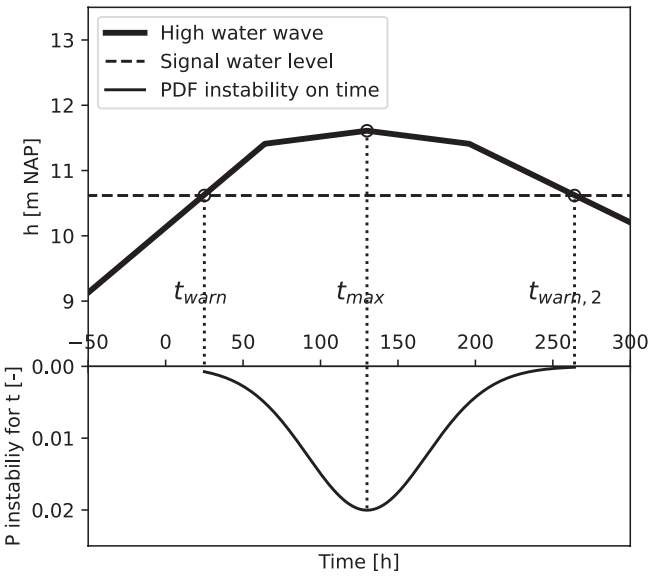

FIGURE 7 | Probability of occurrence of first slope instability, coupled to a typical flood water wave for Rhine river (flood water wave based on Chbab (2016)).

3.4 | Breach Formation Time

The breach formation time, t_{br}, starts either after the damage to the protective grass layer (for overflow) or the reduction in crest level (instability). The total breach formation time is the time required for the breach to develop itself beyond feasible repair. Within the model it is assumed that a levee becomes irreparable once the breach formation advances beyond stage II as defined by Visser (1998). At this stage, the inner slope extends to the outer slope of the levee. After completion of stage II, breach width starts to increase over time (Figure 8, right panel).

This breach formation rate has been found to depend on the water level in the breach, the composition of the levee and the failure mechanism (Janssen et al. 2021). The t_{br} is randomly selected from a normal distribution with a mean of 15 min with a standard deviation of 5 min. These values have also been derived from the real levee failure case Breitenhagen (Brauneck et al. 2016) and the large scale breaching experiment at the Zwin (Visser et al. 1996). These values are valid for erosion of the sand core of the levee. The effect of rising water levels within the breach during the breach process is not taken into account within the model.

4 | Preparation of Emergency Measures: Required Time

4.1 | General Framework

As the times involved with the two selected failure scenarios have been addressed, now the emergency response intervention has to estimated. The application of the emergency measure, *Apply EM*, which requires a time interval of t_{req} to install, is presented in the theoretical framework in Figure 2. Two different flow charts are possible to estimate the total time required: a

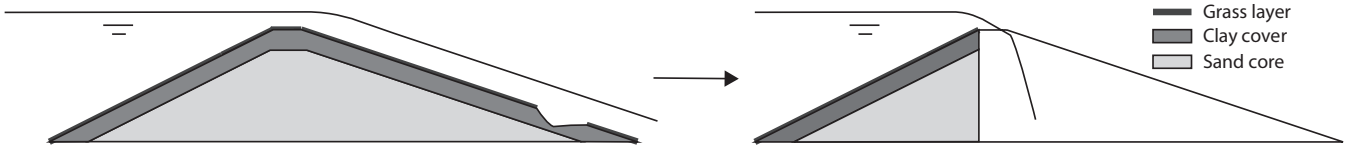

FIGURE 8 | (Left) Cross section at the location of the breach at start of the breach formation process and (right) breach dimensions at the end of stage II, inspired by Visser (1998).

series model (Appendix A) and a parallel model (Figure 9). In the series scheme, all steps in the water crisis event path are modeled consecutively. Whereas in the parallel scheme, the preparation of the emergency measure and the levee inspection process are decoupled, i.e., they are assumed to occur simultaneously in time. The levee inspection process for the Dutch case involves visual inspections for deformations on the levee surface conducted by (trained) personnel. The schematization of both models is derived from emergency guidelines and discussions with experts in flood emergency management in the Netherlands (Knotter and Krikke 2021; MinIenM 2022). The description and schematization of the series model is to be found in Appendix A. The parallel model will now be elaborated further. This model will provide predictions of lower failure probabilities, and is most in line with current practice.

The decoupling of the preparation of the emergency measure and the levee watch, results in three different sub-paths for the parallel scheme (Figure 9). Sub-path I represents the preparation of the levee watch. It starts after a high water signal and ends after detection of damage at the levee (circles). Sub-path II represents the preparation of the emergency measure. It starts following the decision to prepare the measures and ends if material and personal are ready at a storage point (squares). Sub-path III describes the transportation and placement of the emergency measure (triangles). This path starts after completion of both sub-paths I and II. At the end of sub-path III the emergency measure has been successfully installed. The total time, t_{req}, is then given by (Equation 3). The times t_1 to t_6 are the times taken for each branch in the process (Figure 9). The estimated values of times t_1 to t_6 represent a question number in the expert judgment analysis. This is further elaborated in the next section.

$$\begin{aligned} t_{req,par} &= \max\left(t_I, t_{II}\right) + t_{III} \\ t_I &= \max\left(t_1 + t_2, t_{det,dam}\right) + t_{insp} + t_3 \\ t_{II} &= t_4 + t_6 \\ t_{III} &= t_5 + t_{place} \end{aligned} \tag{3}$$

4.2 | Estimation of Time Required: Structured Expert Judgment Analysis

It is challenging to obtain proper estimates for the various process steps for rare and diverse emergency events. In order to obtain as realistic values as possible, experts were interviewed in a systematic manner. In both the series (Figure A1) and parallel

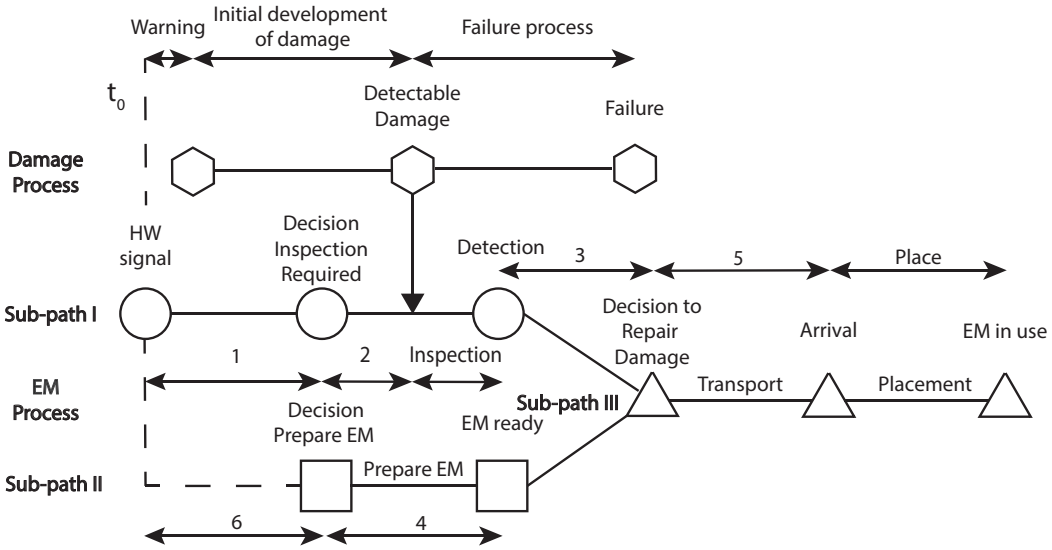

FIGURE 9 | Time required to apply emergency measure (EM), parallel, numbers indicate question in expert judgment (Table 1). The presented case shows being too late.

TABLE 1 | Model parameters as obtained from expert judgment session, question numbers correspond to numbers in Figure 9.

Question	Topic	Sub-path	Unit	5%	50%	95%
1	Decision: Levee watch	I	h	0.3	1.4	7.3
2	Levee watch preparation	I	h	0.6	3.3	11.8
3	Decision: repair required	I	h	0.0	0.5	3.2
4	Preparation emergency measure	II	h	0.5	5.4	12.0
5a	Velocity road transport	III	km/h	17.9	56.2	78.0
5b	Velocity water transport	III	km/h	2.2	5.8	29.3
6	Decision: to apply EM	II	h	0.2	7.8	23.8

(Figure 9) flow diagrams, the steps 1–6 have been labeled. These numbers correspond to a question, as posed in a structured expert judgment analysis, utilizing the classical model developed by Cooke (1991). The questions, directed at the experts, serve as input for the model and are detailed in Appendix B. A total of 22 experts participated in the questionnaire, with the majority being members of the Dutch CTW (Crisis Expertise Team Flood Defences). CTW members work within organizations such as Rijkswaterstaat, Water Boards, Deltares, and Defence. These experts are deployable during a high-water crisis in the Netherlands, mostly by offering expert advice to local water authorities based on their specialized knowledge. The remaining participants have experience with Dutch water safety systems over an extended period of time. The questionnaire was completed on April 19, 2023.

During a 30-min session, the experts were initially briefed on fundamental statistics and the purpose of the expert judgment session. Subsequently, each expert received a paper questionnaire, consisting of 10 calibration questions and 20 questions of interest for estimating the desired parameters. For each question, the experts were requested to provide their estimated 5%, 50%, and 95% quantile answers. The calibration questions were presented on a screen, with supporting background information and visuals. The questions of interest did not contain any extra information. The experts were not allowed to discuss the answers during the session. A complete list of the questions and the anonymized attendees of the questionnaire is to be found in Appendix B.

The expert data has been analyzed with the ANDURYL software package (Rongen et al. 2020), which allows for the analysis of several expert judgment decision makers within a user interface. The output of three decision makers is analyzed. First, the equal decision maker, in which all of the experts responses are weighted equally. Second, the global decision maker, where the weight of the different experts is based on their expert performance. Third, the global optimized, where the most competent experts (which answered the calibration questions best) are selected. The elicitation results of the analysis are presented in Appendix B.

4.2.1 | Expert Output Questions of Interest Within the Model

The results of the expert judgment analysis, determined through the application of the global decision maker, are displayed in Table 1. Additional results and an explanation for choosing this specific decision maker can be found in Appendix B. For each question, a cumulative density function (CDF) can be generated, suitable for employment in the critical time model. Among the inquiries, distinct time frames are addressed. First, those concerning preparation and decision-making related to the levee watch (questions 1, 2, and 3). Second, those addressing the decision to prepare emergency measures (question 4 and 6). Third, those projecting transport velocities during a high water crisis (question 5a and 5b).

4.3 | Inspection

The time required to detect a weak spot after the occurrence, t_{insp}, depends on the speed of inspection of the levee watch and the probability of detecting the damage by the levee watch. A study aimed at measuring the successfulness of the levee inspection during summer inspection gave an average detection probability of $p_{\text{detection}} = 0.7$ per inspection round, for section damages (Klerk et al. 2021). External conditions such as availability of daylight, weather conditions, levee accessibility and experience of the levee watch may influence the detection probability (Bakkenist et al. 2012; CIRIA 2013), but are further neglected here.

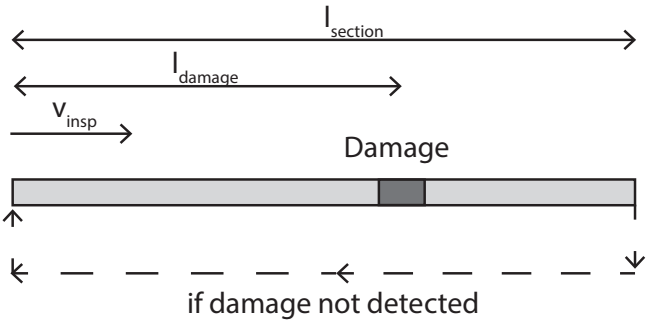

FIGURE 10 | Inspection model, with arbitrary damage location at levee section.

TABLE 2 | Input parameters detection.

Aspect	Value
$p_{\text{detection}}$	0.7 (Klerk et al. 2021)
$l_{section}$	10 km (Knotter and Krikke 2021)
v_{insp}	3 km/h

During levee surveillance, a designated section of the levee is monitored by trained personnel named, the levee watch. The levee watch inspects the section, with a certain length, $l_{section}$, and the inspection is conducted with a certain velocity, v_{insp} (Figure 10). The average $l_{section}$ is set to 10 km (Knotter and Krikke 2021). The parameter v_{insp} is configured to 3 km/h, representing the average walking speed of an adult. The levee watch keeps inspecting the same levee section, for a number of rounds, n_{rounds}, until the damage has been spotted, which is affected the probability of detection, $p_{\text{detection}}$. Within the model, the damage will be located randomly on the levee section, with a distance l_{damage} from the inspector. The total inspection time is the number of rounds times the length of the section, plus the distance to the damage, multiplied by the inspection speed (Equation 4). Inspection values applied within the model are summarized in Table 2. The model only includes the occurrence of a single damage per section.

$$t_{insp} = \frac{n_{rounds} * l_{section} + l_{damage}}{v_{insp}} \tag{4}$$

n_{round} = rounds before decting damage, with probability of succes $p_{\text{detection}}$

4.4 | Transport

The time of transport, t_{trans}, depends on the distance over road (l_{land}) and water (l_{water}) from the storage to the affected levee section, given the respective transportation velocities (Equation 5).

$$t_{trans} = t_5 = \frac{l_{land}}{v_{land}} + \frac{l_{water}}{v_{water}} \quad (5)$$

The standard distances applied in the model are set to a transportation distance of 20 km over land (l_{land}) and 1 km over water (l_{water}) unless stated otherwise. The velocity over land (v_{land}) and water (v_{water}) are randomly selected from the expert judgment results distribution for question 5a and 5b (Table 1). If the model is being applied for land-based emergency measures, the water distance can be disregarded.

4.5 | Placement

In the current model, only the placement of the BresDefender emergency measure is considered. Large scale experiments in the living lab Hedwige-Prosperpolder have been executed to evaluate the placement procedure (Maat et al. 2023). Detailed information on the placement procedure and the conducted experiments can be found in Velde (2022). The mean time required to install the BresDefender after arrival was found to be 46 min with a standard deviation of 10 min (Table 3). The placement time, t_{place}, is a randomly selected value originating from a normal distribution defined by the previous parameters. It should be noted that the time applied in the model is rather conservative; a potential reduction in placement time of at least 15 min is expected to be possible through improvements to the prototype pontoon and enhanced of personnel training (Velde 2022).

In the current placement procedure, the BresDefender can effectively raise the crest height of a levee by 0.3 m. The performance of the BresDefender, when the water level surpasses this threshold remains uncertain. It is anticipated that the pontoon would remain operational, however, more leakage water is expected to flow through the breach, entering frond the sides of the BresDefender. In the model, application of the BresDefender increases the levee height by 0.3 m (h_{em}, Table 3). In the model, it is assumed that the BresDefender consistently raises the levee height by 0.3 m, disregarding the impact of the specific timing requirement for placement within the flood wave. If the river water level surpasses this value, failure occurs. Further improvements to the placement procedure may enlarge the application range and performance, as the maximal water level the BresDefender can stop is determined at 1 m.

5 | Case Studies

Two case study areas are selected to investigate the contribution of several parameters to the probability of success of emergency measures. One case is in the Rhine and the other in the Meuse river basin. These cases represent two different load conditions within the Dutch flood protection system, with a larger warning time for the flood waves in the Rhine compared to the Meuse (Table 4). The Rhine case is located at levee ring 43 at the Waal river branch (Table 4). The Meuse case is located in the Southern part of the Limburg province, near Meers.

TABLE 3 | Placement performances prototype BresDefender emergency measure.

Aspect	Value
mean placement	46 min
std placement	10 min
h_{em}	0.3 m

TABLE 4 | Input parameters for case studies (MinIenM 2022), levee height determined extracted from elevation map, received on June 30th, 2023 (AHN 2023).

	Rhine basin	Meuse basin
River	Waal	Meuse
Levee ring and section	43–5	87–1
Levee reference	DT120.D	0.77
Nearby village	Ochten	Meers
Return period code red (year)	50	50
t_{warn} (h)	24	12
h_{levee} (m above NAP datum)	12.8	37.7
Main failure process	Instability before overflow	Overflow
	Figure 5	Figure 5

The model employs a Monte Carlo analysis, incorporating 10,000 unique values for each individual probability distribution mentioned in the previous chapter. The total times required and available are determined for each unique combination of samples, assessing whether the measure is implemented on time. The structural requirements of the emergency measure are incorporated by adding the additional height to the (reduced) levee height. If the river water level surpasses the total (reinforced) height, assuming the measure was implemented in time, structural failure of the measure will occur within the model.

5.1 | Warning Times

The warning times, which serve as input for the model, are based on the Dutch national procedure for floods (MinIenM 2022). Within this guideline, a return period for a code red in the Rhine river is assumed to be 50 years, while the code red return period for the Meuse is 25–50 years. If a code red is issued, national safety may be at stake. A code red starts 12–48 h before the water level is expected to exceed the signal water level for the Rhine river, and 12 h for the Meuse river (Table 4).

A standard flood wave shape over time for both the Rhine and Meuse case is implemented in the model, following the findings of Chbab (2016). The water levels, corresponding to the selected return period, are determined with Hydra-NL as described by Kolen et al. (2021). The fragility curves providing the probability of a slope instability given a certain water level have been

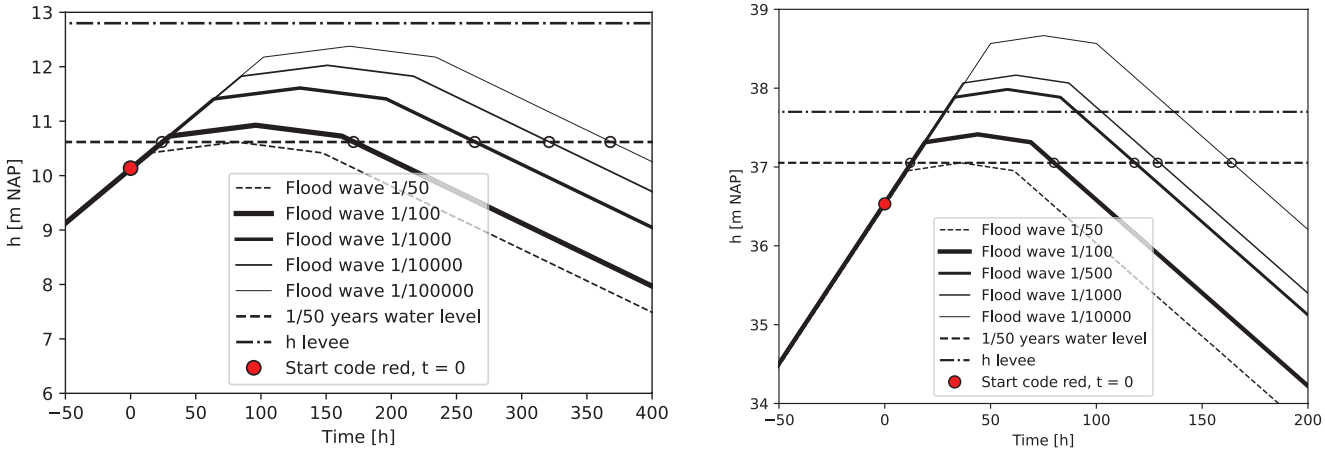

FIGURE 11 | Flood water waves for Rhine (left) and Meuse case (right).

determined with data from OKADER (Kolen et al. 2021). The flood waves for different return periods are plotted in Figure 11.

5.2 | Rhine Case

A conditional and a probabilistic subcase have been implemented for the Rhine river basin case. In the conditional subcase, the model is run given the occurrence of a slope instability (thus the probability of a slope instability is set to 1). In the probabilistic subcase, the fragility curve for slope instabilities determines the probability of this instability. The results of a conditional run for the Rhine case are summarized in Tables 5 and 6, assuming a slope instability leads to a reduction of crest height of 1–2 m. The transportation distance is 20 km over land and 1 km over water. The return period of the high-water wave is 1000 year. In total, 10,000 independent samples are used for the determination of the distributions of the time required and available.

The output in Table 6 indicates that the time required for the levee inspection and to prepare the emergency measure is one order of magnitude smaller than the time required for damage to occur. This indicates that the preparation of the levee watch and the emergency measures is not likely to be a critical step in the process if its preparation begins promptly after the issuing of a code red.

Comparing the failure paths in series (Appendix A) and parallel (Figure 9), a median difference of 6 h in deployment time after issuing code red is observed (Table 5), stemming from the time required to prepare the emergency measure after detection of damage (Table 6) in the series assumption. Table 7 displays the time available before levee failure. The time to overflow refers to the duration between the start of code red and the initiation of overflow over the crest of the levee.

When comparing the median time available until levee failure with the median time required for the series and parallel process, it becomes apparent that the series approach exceeds the available time, while the parallel approach requires approximately the same amount of time as it takes to reach overflow. The conditional probability of being too late ($t_{req} > t_{avail}$) for the serial assumption is 58% while this percentage for the parallel assumption it is 32%. For the remainder of the analysis, only the parallel model will be considered, as it presents the lowest probability of exceeding the time limit.

TABLE 5 | Outcomes for the time required for model runs for the series and parallel schematization, too late is defined as: $t_{req} > t_{avail}$.

	Series	Parallel
Median [h]	134.5	128.5
Standard deviation [h]	40.6	39.6
Probability of being too late [−]	0.58	0.32

Four different steps in the process are important to consider after the occurrence of damage to the levee: detection of damage, the decision to apply the emergency measure, transportation of the measure and the placement of the measure. Detection of damage has the largest expected duration in the post-damage stage (Table 6) followed up by placement of the emergency measure. Reducing the time required for these four steps, will increase the likelihood of being in time and increases the overall performance of the emergency measure (see Section 6). The "fraction of total duration" value in Table 6 is the median value of a step in the period after damage, divided by the total median duration of period after damage.

Figure 12 gives the modeled conditional probability of success, when slope instability occurs, for various return periods of flood waves for the Rhine case. The emergency measure is expected to have a high likelihood of success for events with return periods around 100 years. Notably, the success of the emergency measure decreases as the return period increases. The primary factor contributing to this effect is the increase in the disparity between the river water level and the height of the levee if the return period becomes smaller. The right graph in Figure 12 shows the distribution of outcomes, given levee failure. Both figures show a reduction in the effectiveness of the emergency measure for smaller return periods. The proportion of cases where the emergency measure arrives too late remains relatively constant for the different return periods.

Another observation from Figure 12 is the reduction in success for smaller return periods while the probability of being in time

TABLE 6 | Model results for the Rhine test case for 1/1000 per year conditions, time required in hours, DW = levee watch, EM = Emergency measure.

	Period until damage			Period after damage			
	Prepare DW	Prepare EM	Time to damage	Detect damage	Decision EM	Trans	Place
	Q1 and 2	Q4 and 6	Sect 3	Sect 4.3	Q3	Q5	Sect 4.5
Median [h]	5.2	13.9	120.6	2.4	0.5	0.5	0.8
Standard deviation [h]	18.5	26.5	39.4	2.8	3.1	0.8	0.2
Fraction of total duration after damage [–]				0.50	0.15	0.16	0.18

TABLE 7 | Model results for time available for the Rhine test case.

	Time to overflow	Breach time
Median [h]	126.8	0.3
Standard deviation [h]	34.3	0.1

without success increases, this may indicate the lack of retaining height of the emergency measure for smaller return periods. Figure 13 shows a run of the model with a variable extra height (h_{em}) of the applied emergency measure for a return period of 1/1000 years for the conditional case. This highlights that increasing the height to 0.8 m leads to a significant increase in the likelihood of success. The current BresDefender prototype is able to increase the levee height with 0.3 m above still water level. Considering stability requirements, a maximum retaining height in the order of 1 m is to be found for the emergency measure, thus 0.8 m is in reach.

When considering the complete probabilistic scenario for the Rhine river case, which incorporates the probability of slope instability coupled with the maximum water level in the river based on site-specific fragility curves, it is observed that the probability of success is rather low (Figure 14). This is primarily due to the large share of no failure cases for the lower return periods. The relative success of the emergency measure is similar to the conditional case.

5.3 | River Meuse Case

Model runs were performed for the probabilistic scenario for the Meuse case, which represents a levee prone to overflow (Figure 15). This case represents the probabilistic case, where the probability of a slope failure is determined by a fragility curve, given the water level in the river. The results for a run for a 500 year return period flood wave are given in Table 8, with the probability of a slope instability incorporated as a fragility curve (probabilistic case). This specific return period is selected since the maximum overflowing water depth for this return period is a fraction smaller than the added levee height by the BresDefender, 0.3 m. The estimated probability of being too late for the Meuse case is equal to 1, with the assumption that one starts to prepare the emergency measure after the start of overflow.

The time available until levee failure due to overflow is limited by the 0.3-m height difference between the levee and the river water level in this specific case. The time to install the emergency measure at the right location is too long for all cases if one starts the logistical emergency measure process after the start of overflow.

6 | Discussion

The probabilistic model as described in the previous section includes several assumptions. The first assumption is the overall performance of the prototype BresDefender. During large-scale experiments involving the BresDefender (Maat et al. 2023), leakage water seeping through the pores at the soil-structure interface has been noted. However, the observed amount of leakage water is not expected to lead to severe damage progression. Furthermore, in the model, a water level exceeding the increased crest level is incorporated as failure; however, in reality, the emergency measure reduces the flow potential and herewith increases the time to failure. This will improve the overall performance of the levee. The exact effect on the breaching time needs further research.

A second assumption is neglecting spatial variations in levee properties: the resistance of the grass varies spatially in crest direction; the presence of e.g., animal burrows may decrease the resistance of a levee locally (Koelewijn et al. 2022). This effect is not taken into account within the model. These irregularities of the levee cross section do explain the relatively large standard deviation in the occurrence of damage.

The case studies applied in the manuscript are cases within the Dutch river system; however, the presented model can be applied to cases outside of the Netherlands as well. Applying this model outside the Netherlands requires site-specific information of the location of interest. Additionally, the current model only incorporates the damage processes overflow and instability; however, the same modeling approach can be applied to other failure processes, e.g., piping.

6.1 | Proactive Applying Emergency Measures

The essential parameter contributing to the failure of emergency measures is being too late, i.e., the damage of the levee

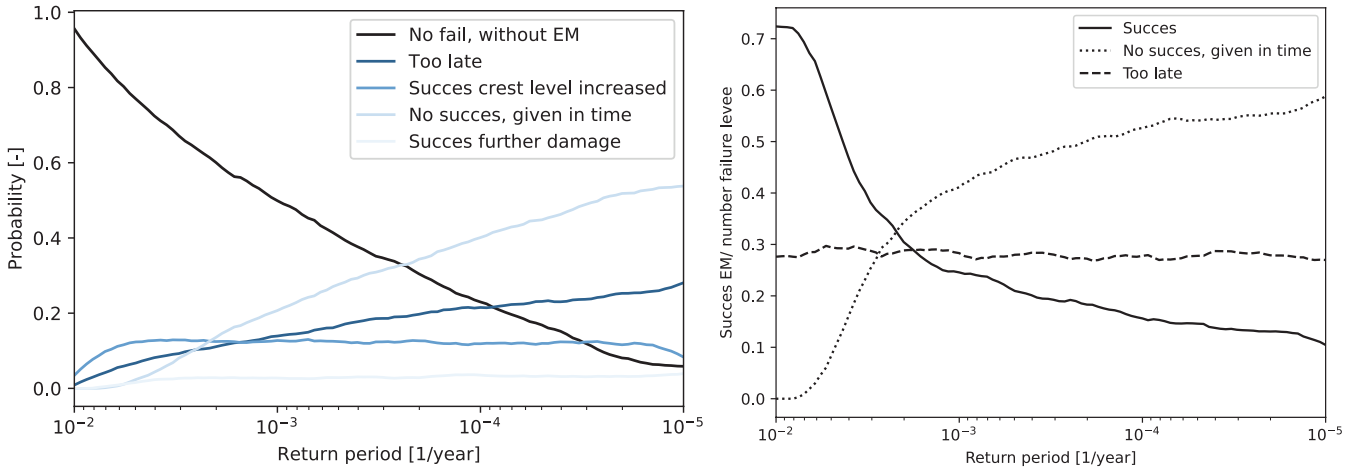

FIGURE 12 | (Left) Conditional probability of successful mitigation by emergency measure (EM) for the Rhine case, given slope instability and (right) relative success rate of emergency measures, where the relative value is the variable divided by the number of levee failures. The base case can be extracted from the right figure.

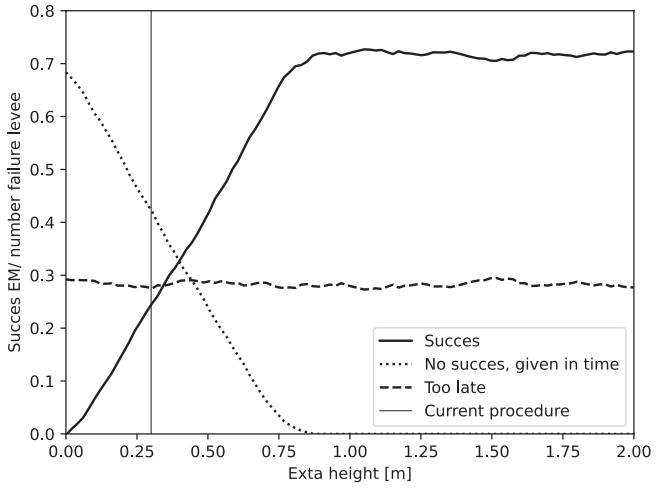

FIGURE 13 | Effect retaining height measure (h_{em}) on success rate emergency measure (EM), Rhine river, return period 1/1000 years.

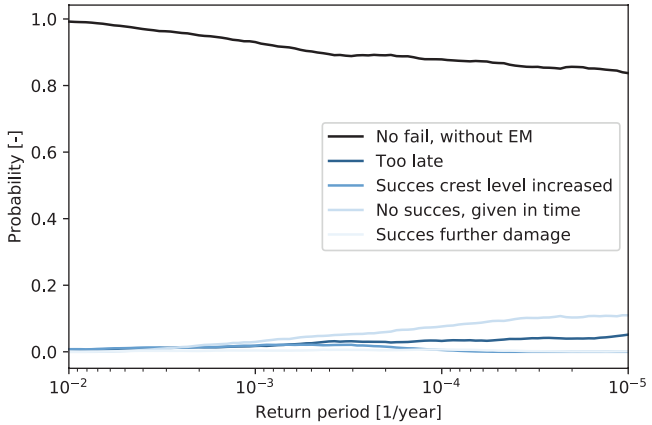

FIGURE 14 | Results of the full probabilistic run for the Rhine case.

already progressed beyond a repairable level before preparation of the emergency measure. This preparation includes the steps of detection of damage, the decision to repair the damage, the transport of emergency measures to the weak spot, and proper placement.

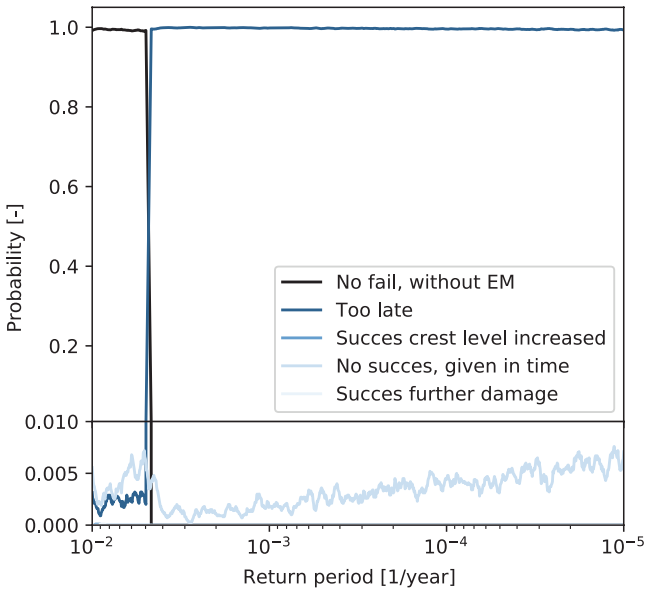

FIGURE 15 | Probabilistic probability of failure for Meuse case.

Possible improvements in the application of an emergency measure after the detection of damage include better detection of the damage, in particular by sensors in the levee (Schenato 2017), or monitoring by drones (Shoemaker et al. 2019) and satellites (Özer et al. 2018). Transportation and placement of the emergency response measure BresDefender can be improved by faster transportation, for example airborne. Creating a denser network of more storage places will also reduce the transportation time to the site. Another possibility is to decrease the placement times by improving the current BresDefender prototype. This includes both training of personnel and structural improvements to the physical system.

The impact of reducing the duration of these steps on the probability of being too late is depicted in Figure 16 (return period 1000 years, standard Rhine parameters and return period 500 years, standard Meuse parameters). For the Rhine case, the probability of being too late reduces almost linearly for increased reduction factor, ultimately approaching zero for a 100%

TABLE 8 | Outcomes run model for series and parallel run data for the period after damage is equal to data in Table 6.

	Time available			Time required	
	Time to overflow	**Resistance overflow**	**Breach time**	**Series**	**Parallel**
Median [h]	29	1.2	0.3	38.9	32.9
Standard deviation [h]	0.2	0	0.1	17.1	25.6
Probability of being too late [–]				1	1

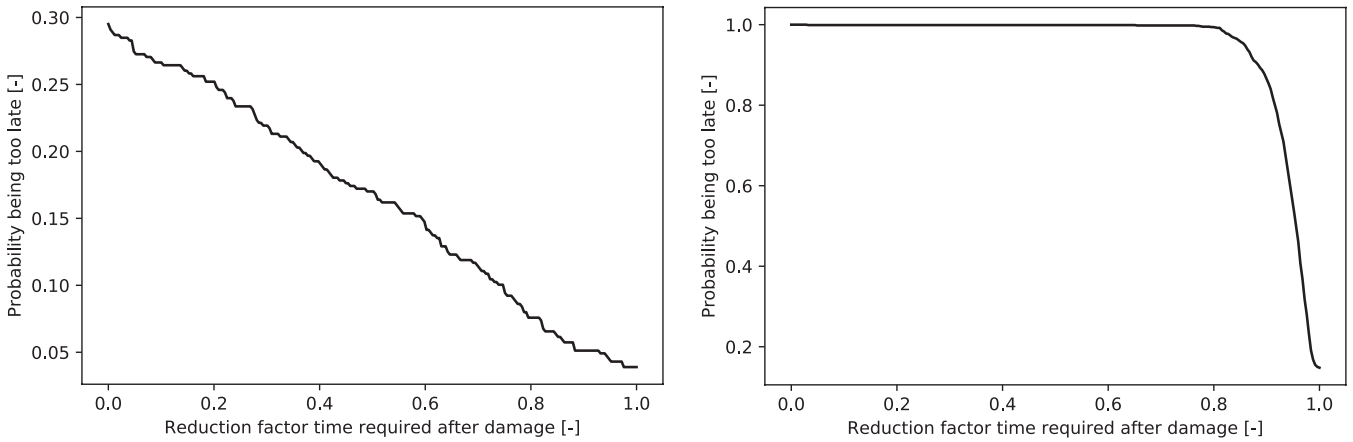

FIGURE 16 | Reduction probability too late by reducing time required after occurrence of damage (left) for the standard Rhine river basin case and (right) for the standard Meuse river case.

reduction factor. Reducing the time required by 50% may decrease the probability of failure to 17%. For the Meuse case, a reduction in the probability of being too late is only achieved when reducing the time required by more than 90%. This reduction in being too late can only be achieved by proactively sending the emergency measure to a spot on the levee, where future damage is to be expected. The median time required after damage is 3.2 h, without the reduction factor. However, reducing the time required by 90% requires measures that could not be classified as emergency measures anymore.

6.2 | Implicit Assumptions Within the Model

Within the presented model, it is implicitly assumed that the high water prediction models lead to perfect predictions of the flood water wave. Next to that, it is assumed that the levee managers do not make wrong decisions within the crisis process. Incorporating these aspects with corresponding uncertainties into the model may decrease the overall performance of the emergency measure. These wrong decisions will reduce the probability of success by the same percentage as the probability of making a wrong decision.

A second implicit assumption within the model is a conservative estimation of the overflow velocity, which is only determined as the maximum difference between levee height and river water level and does not include a time component. Incorporating a more detailed description for the grass resistance will result in more time to overflow and a higher performance of overflowing cases.

7 | Conclusions

A model to estimate the overall performance of emergency measures and specifically the BresDefender, to locally increase the residual strength of a levee in case of a high water crisis has been developed. The approach presented allows for the identification of critical subprocesses in the preparation of emergency measures, particularly those that require significant time and therefore contribute the most to unsuccessful deployments. Model runs have been performed for two cases within the Dutch water system, one at the Rhine river basin and one at the Meuse river basin. An expert judgment assessment study has been conducted to estimate the time required to deploy an emergency measure at a weakened levee section.

The probability of successful application of an emergency measure is mainly dependent on the amount of time required from the occurrence of damage until the installment of the emergency measure. In this timeframe, the detection of damage, the decision to repair that damage, the transport of the emergency measure to the weakened spot, and the placement of the emergency measure are included. According to the model, there will be sufficient time to prepare both people and materials before the occurrence of damage if the authorities embed these steps in the flood safety system. This conclusion results from a comparison of both a series and parallel logistical approach.

For the case study for the Rhine river, assuming a slope instability, the conditional expected probability of being too late is 30% for all considered return periods. Reducing the time required after the occurrence of damage (mainly by decreasing the time

required to detect a damage) by 50% may decrease the failure rate to 17%. The unconditional success rate of the BresDefender is 1.5%; this percentage is relatively low, caused by the high share of no levee failure.

The primary finding of the Meuse case study is that, following an overflow event, there is a limited window of opportunity, often just a few hours, to implement emergency measures. This results in a relatively low probability of success for the application of the BresDefender.

An important finding is the need to act proactively if extreme water levels are expected; this is expected to increase the successfulness of emergency measures. One recommendation is to couple the preparation of an emergency measure to a high water alarm; this reduces the time required to bring an emergency measure to a weak spot after the occurrence of damage. A second recommendation is proactively bringing an emergency measure toward a specific levee section before the detection of damage. This requires substantial knowledge of the levee system and its potential weak spots as well as earlier detection.

The time required for detection of damage is the most critical step within the model. Innovative measures for levee inspection could increase the inspection speed and herewith reduce the time required to detect a damage after its occurrence. Possible improvements could be the monitoring of damages with satellites or sensors.

More research on the BresDefender emergency measure is advised. Further research should test methods to increase its retaining height. An optimized installation procedure could increase the achieved retaining height of the BresDefender to the full potential of 1 m. This will increase the range of return periods in which the emergency measure can be applied. Furthermore, optimization of the placement procedure is recommended to decrease the operation time, as measured during the pilot test of the BresDefender.

Overall, emergency measures are expected to be a valuable asset to locally increase the residual strength of a levee in case of expected levee failure. The overall success rate of emergency measures is expected to decrease for events with smaller return periods. Embedding emergency measures within high-water emergency procedures will reduce the uncertainty in the estimated required time of application together with a reduction in the probability of being too late.

Acknowledgments

The research was funded by the Dutch Ministry of Defence. The large-scale experiments in the Hedwigepolder were part of the Interreg Polder 2C's project (www.p2cs.eu). The authors would like to thank the experts of the Collaboration Crisis Expertise Flood Defences (CTW) for their input for the expert judgment analysis. At last, the support of all students involved in the study is highly appreciated.

Conflicts of Interest

The authors declare no conflicts of interest.

Data Availability Statement

The data that support the findings of this study are openly available in 4TU.ResearchDataat http://doi.org/10.4121/152663fc-0e02-46bf-a0c7-2ebb7b509f68 (Janssen 2023).

References

AHN. 2023. Actueel Hoogtebestand Nederland. Retrieved from. https://www.ahn.nl/.

Bakkenist, S., O. van Dam, A. van der Nat, F. Thijs, and W. de Vries. 2012. Principles of Professional Inspection—Organizational Part. Retrieved from STOWA.nl.

Brauneck, J., R. Jüpner, R. Pohl, and F. Friedrich. 2016. *Auswertung Des Deichbruchs Breitenhagen (Juni 2013) Anhand von UAS-Basierten Videoaufnahmen. Gewässerentwicklung & Hochwasserrisikomanagement-Synergien, Konflikte Und Lösungen Aus EU-WRRL Und EU-HWRM-RL(57)*, 119–128. Technische Universität Dresden, Institut für Wasserbau und technische Hydromechanik.

Chbab, H. 2016. Waterstandsverlopen Rijntakken en Maas Wettelijk Toetsinstrumentarium WTI-2017. Retrieved from Deltares.

CIRIA. 2013. *The International Levee Handbook*. CIRIA. Retrieved from CIRIA document nr C731, London, downloadable through ciria.org.

Cooke, R. 1991. *Experts in Uncertainty: Opinion and Subjective Probability in Science*. Oxford University Press, USA.

Delfland. 2011. *Calamiteitenbestrijdingsplan Regionale en overige waterkeringen*. Hoogheemraadschap van Delfland. Retrieved from Wiki noodmaatregelen.

Henning, B., and R. Jüpner. 2015. "Deichbruch Fischbeck—zwei Jahre danach." *Wasser Und Abfall* 17, no. 11: 15–19. https://doi.org/10.1007/s35152-015-0576-6.

Hewlett, H., L. Boorman, M. Bramley, and E. Whitehead. 1985. *Reinforcement of Steep Grassed Waterways. CIRIA Report, TN 120*. CIRIA (Construction Industry Research and Information Association).

Hoogwater, T. F. F. F. 2021. *Hoogwater 2021 Feiten en Duiding. ENW Report*. https://doi.org/10.4233/uuid:06b03772-ebe0-4949-9c4d-7c1593fb094e.

Janssen, D. 2023. "Data Underlying the PhD Thesis: BresDefender, An Experimental Study on an Emergency Response Measure for Levee Breaches." *Version 1. 4TU.ResearchData.Dataset*. https://doi.org/10.4121/152663fc-0e02-46bf-a0c7-2ebb7b509f68.v1.

Janssen, D., A. J. M. Schmets, B. Hofland, E. Dado, and S. N. Jonkman. 2021. "BresDefender: A Potential Emergency Measure to Prevent or Postpone a Dike Breach." In *Proceeding, FLOODrisk2020: 4th European Conference on Flood Risk Management*. EDP Sciences. https://doi.org/10.3311/FloodRisk2020.19.3.

Jonkman, S. N. 2007. *Loss of Life Estimation in Flood Risk Assessment: Theory and Applications*. (PhD thesis). Delft University of Technology.

Klerk, W. J., W. Kanning, M. Kok, J. Bronsveld, and A. R. M. Wolfert. 2021. "Accuracy of Visual Inspection of Flood Defences." *Structure and Infrastructure Engineering* 19, no. 8: 1076–1090. https://doi.org/10.1080/15732479.2021.2001543.

Knotter, H., and A. Krikke. 2021. Crisisbestrijdingsplan van Waterschap Rivierenland, Hoogwater Retrieved from Wiki Noodmatregelen.

Koelewijn, A. R., S. J. H. Rikkert, P. Peeters, D. Depreiter, M. van Damme, and W. Zomer. 2022. "Overflow Tests on Grass-Covered Embankments at the Living Lab Hedwige-Prosperpolder: An Overview." *Water* 14, no. 18: 2859. https://doi.org/10.3390/w14182859.

Kolen, B., J. Caspers, and J. Pol. 2021. Actualisatie OKADER, Voor toepassing bij de IRM-MER. Retrieved from Rijkswaterstaat.

Kool, J. J., W. Kanning, T. Heyer, C. Jommi, and S. N. Jonkman. 2019. "Forensic Analysis of Levee Failures: The Breitenhagen Case." *International Journal of Geoengineering Case Histories* 5, no. 2: 70–92.

Koopman, R. 2022. Landmacht Docu: Terugblik inzet landmacht militairen Hoogwater Limburg 2021. https://www.youtube.com/watch?v=IIL7DJ1Ts_k&t=160sKoninklijkeLandmacht.

Kundzewicz, Z. W., S. Kanae, S. I. Seneviratne, et al. 2013. "Flood Risk and Climate Change: Global and Regional Perspectives." *Hydrological Sciences Journal* 59, no. 1: 1–28. https://doi.org/10.1080/02626667.2013.857411.

Lendering, K. T. 2018. *Advancing Methods For Evaluating Flood Risk Reduction Measures*. (PhD thesis). Delft University of Technology.

Maat, W. H., M. L. M. Balemans, A. J. M. Schmets, and D. Janssen. 2023. Pilot Breach Defender (BresDefender) (D.2.1.1). Retrieved from. www.polder2cs.eu.

MinIenM. 2022. Landelijk Draaiboek Hoogwater en Overstromingsdreiging. Retrieved from Rijkswaterstaat.

Nat, v. d. A. 2012. Hoogwaterklapper noodmaatregelen Retrieved from Waterschap Groot Salland.

Özer, I. E., F. J. van Leijen, S. N. Jonkman, and R. F. Hanssen. 2018. "Applicability of Satellite Radar Imaging to Monitor the Conditions of Levees." *Journal of Flood Risk Management* 12, no. S2: e12509. https://doi.org/10.1111/jfr3.12509.

Peeters, P., G. Zhao, L. De Vos, and P. J. Visser. 2014. "Large-Scale Dike Breaching Experiments at Lillo in Belgium. In 2015)." In *Proceedings of the 7th International Conference on Scour and Erosion Y ICSE, 289Y297*.

Remmerswaal, G., P. J. Vardon, and M. A. Hicks. 2021. "Evaluating Residual Dyke Resistance Using the Random Material Point Method." *Computers and Geotechnics* 133: 104034. https://doi.org/10.1016/j.compgeo.2021.104034.

Rijkswaterstaat. 1961. Verslag over de stormvloed van 1953. Retrieved from TU Delft repository.

Rijskwaterstaat. 2023. Rijkswaterstaat Waterinfo Extra. Retrieved from. https://waterinfo.rws.nl/.

Rongen, G., C. M. P. t. Hart, G. Leontaris, and O. Morales-Nápoles. 2020. "Update (1.2) to ANDURIL and ANDURYL: Performance Improvements and a Graphical User Interface." *SoftwareX* 12: 100497. https://doi.org/10.1016/j.softx.2020.100497.

Schenato, L. 2017. "A Review of Distributed Fibre Optic Sensors for Geo-Hydrological Applications." *Applied Sciences* 7, no. 9: 896. https://doi.org/10.3390/app7090896.

Schiereck, G. 1998. Grondslagen voor waterkeren. Report, Rijkswaterstaat, 1998b. Retrieved from TU Delft Repository.

Shoemaker, T. A., M. P. McGuire, and G. Roussel. 2019. "Remote Sensing Approach to Upstream Slope Inspection." *Journal of Geotechnical and Geoenvironmental Engineering* 145, no. 11: 04019102. https://doi.org/10.1061/(asce)gt.1943-5606.0002159.

t Hart, R., H. De Bruijn, and G. De Vries. 2016. Fenomenologische beschrijving Faalmechanismen WTI Retrieved from Deltares.

Van Der Krogt, M. G., T. Schweckendiek, and M. Kok. 2019. "Do all Dike Instabilities Cause Flooding?." In *13th International Conference on Applications of Statistics and Probability in Civil Engineering (ICASP13), Seoul, South Korea, May 26–30, 2019*. https://doi.org/10.22725/ICASP13.461.

Van, M. A., E. Rosenbrand, R. Tourment, P. Smith, and C. Zwanenburg. 2022. "Failure paths for levees. International Society of Soil Mechanics and Geotechnical Engineering (ISSMGE) – Technical Committee TC201 'Geotechnical Aspects of Dikes and Levees' Download." https://doi.org/10.53243/R0006.

Velde, R. A. S. v. d. 2022. *Optimalisatie plaatsingsmethode BresDefender*. (BSc thesis). Netherlands Defence Acedemy, Den Helder.

Visser, P. J. 1998. *Breach Growth in Sand-Dikes*. (PhD thesis). Delft University of Technology.

Visser, P. J., M. J. Smit, and D. W. Snip. 1996. "Zwin'94 Experiment; Meetopstelling en Overzicht van alle Meetresultaten." *Technical Report, 4-96, Vakgroep Waterbouwkunde, Fac. Civiele Techn., Techn. Univ. Delft, Delft, The Netherlands*.

Appendix A

Series Model

In this appendix, the series model is elaborated on. Within the series model it is assumed that emergency response measures are only prepared after detection of a damage to the levee. This sequence begins with a high water signal, after which a decision is made to intensify the levee watch on the levee. Levee inspectors start to inspect the levee until a damage is detected. After detection of the damage, a decision has to be made on the required emergency measure. This decision results in preparation of the emergency measure in terms of material and personnel. Then, the measure is transported from storage to the damaged levee section. At last, the emergency measure is placed, ready to fulfil its purpose. The total time required ($t_{req,ser}$) is the sum of all the steps in the scheme (t_{path}) (Equation A1). The numbers t_1 to t_5 are defined in Figure A1.

$$t_{req,ser} = \max\left(t_1 + t_2, t_{det,dam}\right) + t_{insp} + t_3 + t_4 + t_5 + t_{place} \quad \text{(A1)}$$

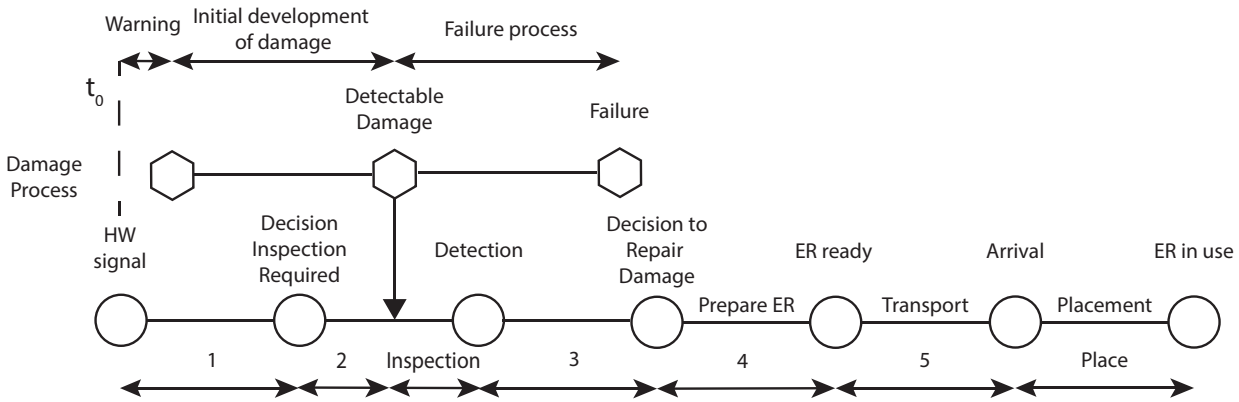

FIGURE A1 | Time required to apply emergency measure (EM), steps in series, numbers indicate question in expert judgment (Table B1).

Appendix B

Expert Judgment

This appendix shows the results of the expert judgment session, as conducted on the 30th of April 2023. The questions asked to the experts are show in Table B1. The participants of the expert judgment session are not made available here, for privacy reasons. The attendees are arranged in alphabetical order, with randomly assigned expert IDs as employed within the analysis. The overall performance of the experts is shown in Table B2. The calibration scores of 18 out of the 22 experts is smaller

TABLE B1 | Questions expert judgment session.

Number	Question	Realization	
1	Arrival military in Sitard during floodings in Limburg, 2021 (Hoogwater 2021; Koopman 2022)	6.5	h
2	Placement sandbags at levee which suffered macro instability at Fishbeck 2014 (Henning and Jüpner 2015)	6	h
3	Failure levee after detection first damage, Fishbeck 2014 (Henning and Jüpner 2015)	17	h
4	Time first water till failure in experiments Lillo 2015 (Peeters et al. 2014)	30	min
5	Expected return period of a code red at Lobith (MinIenM 2022)	50	year
6	Discharge of Rhine at Lotith on the 26th of April 2023 at noon (question was asked the 19th of April around noon) (Rijskwaterstaat 2023)	2202	m^3/s
7	Width of the breach which was enclosed, using the vessel "de twee gebroeders" during the Dutch Watersnoodramp in 1953 (Rijkswaterstaat 1961)	6.5	m
8	Initial discharge through breach initiated with explosives during experiments in Marnewaard, 2023 (own dataset)	1.46	m^3/s
9	Placing 1 row of sandbags over a length of 100 m (Nat 2012)	8	min
10	Evacuation of 237 people out of hospital Venlo, during the Limburg flood in 2021 (Hoogwater 2021)	10	h
11 (1)	How much time do you think is needed between receiving a high-water alarm, code red, and the decision to intensify levee surveillance?		
12	What is your estimate of this time for a code orange?		
13	What is your estimate of this time for a code yellow?		
14 (2)	How much time do you expect it will take for the levee watch to become operational on location after the decision to 'intensify the levee watch' has been made?		
15 (6)	How much time do you think is needed between receiving a high-water alarm code red and the decision to prepare emergency measures?		
16	What is your estimate of this time for a code orange?		
17	What is your estimate of this time for a code yellow?		
18 (4)	How much time after giving the signal to prepare emergency measures do you expect the emergency measures to be ready for transport, when using civilian resources (both personnel and equipment), in general?		
19	Using sandbags?		
20	Using Bigbags		
21	How much time after giving the signal to prepare emergency measures do you expect the emergency measures to be ready for transport, when using military resources (both personnel and equipment), in general?		
22	Using the BresDefender		
23	Using explosives		
24 (5a)	What do you estimate the average speed is for transporting emergency measures by road to the required location during a high-water crisis?		
25 (5b)	By transport over water		
26 (3)	How much time do you expect is needed between the discovery of a significant levee damage and the decision to repair the damage, under code red?		
27	What is your estimate of this time for a code orange?		
28	How much time do you think can be gained through informal channels before the high-water alarm is officially given, during a high-water event from the Rhine river (3+ days before the peak, with accurate prediction)		
29	How much time do you think can be gained through informal channels before the high-water alarm is officially given, during a high-water event from the Meuse river (1 day before the peak, with accurate prediction)		
30	How much time do you expect to start transporting materials to the location after detecting actual damage at a recognized weak spot in the levee?		

than 1×10^{-2}. This is a rather low score for most of the experts, where scores close to or higher than one are to be expected. This suggests a potential misalignment between the calibration questions and the expertise of the experts. The calibration questions encompassed estimations of discharges and velocities of river flows, which differs from the unit of time requested in the questions of interest. A comparison between the mean values of the questions of interest for the equal decision maker (all experts are weighted equally) and the global decision maker (the weight of the experts is based on the performance of the calibration questions) reveals that the weighted mean values for the equal and global decision maker are in the same order of magnitude. However, the uncertainty intervals are broader for the equal decision maker. Consequently, it can be inferred that all experts are converging toward the values postulated by the best experts. Given this observation, the global decision maker is applied, to include the best experts, but do not exclude the experts who perform bad in the calibration questions.

TABLE B2 | Calibration, information and weight scores experts.

ID	Cali	Info real	Info tot	Weight (Global)	Weight (Global_opt)
Exp A	1.7×10^{-4}	3.706	2.629	7.12×10^{-4}	0
Exp B	0.037	3.691	3.564	0.151	0.184
Exp C	7.4×10^{-4}	4.044	4.090	3.32×10^{-3}	0
Exp D	0.121	3.786	3.339	0.509	0.616
Exp E	3.7×10^{-6}	4.506	3.876	1.87×10^{-5}	0
Exp F	2.2×10^{-4}	3.515	3.253	8.41×10^{-4}	0
Exp G	4.7×10^{-4}	4.287	4.156	2.25×10^{-3}	0
Exp H	0.037	4.092	3.301	0.168	0.200
Exp I	0.020	4.112	3.256	0.090	0
Exp J	3.1×10^{-3}	3.199	3.140	0.011	0
Exp K	1.1×10^{-3}	3.818	3.928	4.66×10^{-3}	0
Exp L	4.0×10^{-5}	3.666	3.599	1.63×10^{-4}	0
Exp M	3.2×10^{-5}	3.010	2.236	1.08×10^{-4}	0
Exp N	1.7×10^{-3}	2.323	1.924	4.31×10^{-3}	0
Exp O	1.7×10^{-4}	4.210	3.797	8.09×10^{-4}	0
Exp P	2.0×10^{-5}	3.926	3.639	8.89×10^{-5}	0
Exp Q	4.7×10^{-4}	3.605	3.445	1.89×10^{-3}	0
Exp R	1.7×10^{-4}	3.703	3.287	7.12×10^{-4}	0
Exp S	1.7×10^{-4}	3.143	3.247	6.04×10^{-4}	0
Exp T	4.9×10^{-3}	4.285	3.841	0.023	0
Exp U	2.8×10^{-9}	3.633	2.879	1.13×10^{-8}	0
Exp V	8.3×10^{-3}	2.992	2.481	0.028	0
Global	0.640	2.506	2.111		
Global_opt	0.754	4.008	3.619		
Equal	0.190	1.950	1.707		